Effects of High CO2 Contents on the Biogas/Diesel RCCI Combustion at Full Engine Load

Ibrahim Babangida Dalha
Centre for Automotive Research and Electric Mobility (CAREM), Universiti Teknologi PETRONAS

Mior Azman Said
Centre for Automotive Research and Electric Mobility (CAREM), Universiti Teknologi PETRONAS

Zainal Ambri Abdul Karim
Centre for Automotive Research and Electric Mobility (CAREM), Universiti Teknologi PETRONAS

Salah El-din Mohammed
Centre for Automotive Research and Electric Mobility (CAREM), Universiti Teknologi PETRONAS

https://doi.org/10.5109/4774216

出版情報：Evergreen. 9 (1), pp.49-55, 2022-03. Transdisciplinary Research and Education Center for Green Technologies, Kyushu University
バージョン：

Effects of High CO_2 Contents on the Biogas/Diesel RCCI Combustion at Full Engine Load

Ibrahim Babangida Dalha[1,2,*], Mior Azman Said[1,*], Zainal Ambri Abdul Karim[1] and Salah El-din Mohammed[1]

[1]Centre for Automotive Research and Electric Mobility (CAREM), Universiti Teknologi PETRONAS, Banda r Seri Iskandar 32610, Perak, Malaysia

[2]Faculty of Engineering, Ahmadu Bello University, Samaru 1045, Zaria, Nigeria

*Author to whom correspondence should be addressed:
E-mail: Ibrahim_16005836@utp.edu.my, p20420@abu.edu.ng, miorazman@utp.edu.my

(Received September 28, 2021; Revised March 15, 2022; accepted March 23, 2022).

Abstract: Disparities in the constituents among biogases pose various control challenges during combustion, thus complicating its operability. Improving biogas by eliminating carbon dioxide (CO_2) remains difficult, and high CO_2 concentration is known to affect combustion. Still, the effect on Biogas/Diesel dual-fuel reactivity-controlled compression ignition (RCCI) combustion is not well explored. The influence of high diluent (CO_2) proportions (25 – 45%) and Biogas fraction (40 – 70%) on Biogas/Diesel dual-fuel RCCI combustion was evaluated experimentally, at full load and 1600 rpm. The results show distinct temperature trends across the combustion regimes for all the CO_2 ratios and Biogas fractions. The radiation absorption effect of high CO_2 reduces the cylinder temperature and delays the expansion to a 10 – 20° crank angle after the top dead centre (CA ATDC). The temperature and pressure decrease with the increase in CO_2 ratios and Biogas fractions, unlike heat released rate. Burning Diesel and 45% CO_2 indicate the fastest combustion, with combustion phasing (CA50) at 6.353 ms ATDC while 25 and 35% CO_2 were slowed by 0.258 and 0.578 ms, respectively. Inferentially, 35% CO_2 at a fraction of 50% could form the best reactivity.

Keywords: RCCI combustion; high CO_2 content; biogas

1. Introduction

The use of alternative fuel alongside fossil energy demonstrated a considerable potential to address some combustion and global emissions challenges through the invention of more efficient technologies[1)], such as reactivity-controlled compression ignition (RCCI). In RCCI combustion, different fuels of varying reaction rates get instant blending in the cylinder to enhance the combustion magnitude through layer formation[2-4)]. Self-ignition of a fuel having a high reaction rate initiates the combustion causing a subsequent burning of low reactive fuel due to the rise in the temperature and pressure in RCCI combustion[5)]. Gaseous fuel utilization is among the measures taken to address some RCCI combustion shortcomings[6)]. Still, minimal attention is given to the use of biogas[7)].

Biogas could be obtained through the anaerobic digestion of organic compounds[8)]. Biogas composes single carbon alkane (methane, CH_4), diluent (carbon dioxide, CO_2), some nitrogen elements and other objectionable detrimental compounds like silicon oxides, hydrogen sulfide, and ammonia. Utilizing biogas would curtail the vigorous trend of fossil energy and reduce its global impacts[9)]. It supplies power for domestic appliances as well as internal combustion engines. The impurities are mainly a factor of biogas source and could be harmful to combustion engines[10)]. The constituent's disparities pose various control challenges during combustion, thus complicating its operability[11)]. Biogas unsteady combustion characteristics affect its utilization rate[12,13)]. Gaseous fuel and diesel combustion also produce high emissions[14)]. These deficiencies have encouraged more search and testing of biogas in RCCI mode.

Previous efforts on various synthetic biogas compositions utilized in RCCI combustion do not reflect raw biogas. Wang et al.[15)] study the attributes of low-quality biogas constituting 5% CH_4, 5% 40% carbon monoxide (CO), hydrogen gas (H_2), and 50% nitrogen gas (N_2) as similarly reported by[15)]. Also, Kakaee et al.[17)] evaluate the effects of biogas containing high CH_4 and nitrogen gas with 0.28% CO_2 in RCCI mode. Carbon dioxide pollutant also mainly come from the combustion of gaseous fossil fuels as a power source[17], besides other types[19)]. According to Hosseini and Wahid[20)], the process of improving biomass-based biogas in eliminating CO_2

remains expensive. The difficulties in enhancing biogas by eliminating CO_2 and the diverse disparities in the constituents among biogases used in RCCI combustion motivate the authors to investigate the influence of high CO_2 proportion in biogas. Most of the research on the impact of diluent concentration focuses on lab-scale conditions with high pre-heating temperature and pressure, mainly covering the output from shock tube analysis, rapid compression machines, and continuous flow reactors for biogas combustion, but not in RCCI mode. Quintino et al.[21] opine that some diluent types evaluated might not conform to biogas combustion in an atmospheric scenario; thus, they require intense efforts in more practical settings.

The article,[22], published on the effects of port injection at the valve and various engine capacities, at a 25% CO_2 proportion, indicates an upper maximum temperature at full engine load (6.5 bar IMEP, indicated mean effective pressure). Although there have been numerous studies on the use of biogas in SI and advanced dual-fuel CI engines such as RCCI, few studies are available on the effect of biogas with high CO_2 content for enhanced combustion output. Therefore, this paper investigates the effects of various high CO_2 portions on energy efficiency to enhance the power generated in biogas-diesel RCCI engine at full load and speed of 1600 rpm in a premixed mode experimentally.

2. Theory/Calculations

2.1 Cylinder temperature measurement

The temperature was measured from the cylinder pressure (P) and volume (V) data obtained at various crank angle (θ) positions (i) using Eq. 1 [2,23].

$$T_g = \frac{P_i V_i w_a}{m_a R} \qquad (1)$$

In Eq. 1, T_g is the cylinder gas temperature at a crank angle i (K), w_a is the air molar weight (28.9 g/mol), m_a represents the intake airflow mass (g/s), and R represents the gas constant (8.314 J.mol-1K-1). The mass of intake air was calculated using the generic speed-density method shown in Eq. 2 [3,24].

$$m_a = \frac{w_a V_d \eta_{vol} (p_{abs} - (\frac{p_{atm}}{CR})}{R T_a} \qquad (2)$$

In Eq. 2, η_{vol} represents the volumetric engine efficiency (0.95), p_{abs} represents absolute pressure at intake manifold (kPa), and p_{atm} represents barometric pressure (kPa). CR stands for compression ratio, and T_a is the intake manifold charge temperature (K).

2.2 Cylinder heat released measurement

The heat release rate (HRR) was determined using an empirical model (Eq. 3) developed by applying the first law of thermodynamic[25].

$$\frac{dQ_{net}}{d\theta} = \frac{\gamma}{\gamma-1} P \left[\frac{dV}{d\theta}\right] + \frac{1}{\gamma-1} V \left[\frac{dP}{d\theta}\right] \qquad (3)$$

In Eq. 3, Q_{net} is the net heat release rate (kJ/CA), and γ is a polytropic index estimated from the cylinder pressure readings for best fit[6].

3. Methodology

3.1 Measurement and experimental settings

The work investigates the influence of port-injected biogas with a high CO_2/CH_4 ratio and direct-injected Diesel on the RCCI combustion at full engine load experimentally. The port injection of biogas was at a distance of 115 mm from the inlet valve position to ensure proper air-biogas mixing before entering the combustion chamber, as shown in Fig. 1. The biogas pressure was decompressed to 2 bar using a Linde HiQ pressure regulator. The 2 bar biogas injection pressure for this test was arbitrarily selected based on the information from the literature. Other details of the experimental setup could be seen in the article[2,22]. Table 1 shows the specification of the test engine.

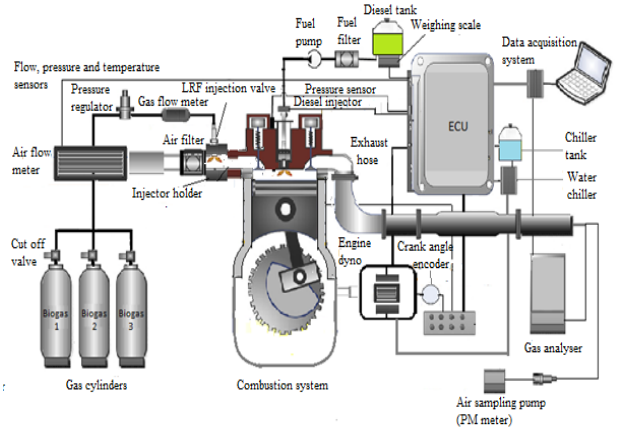

Fig. 1: Schematic of the engine test rig[3].

3.2 Experimental procedure

Experiments were carried out to investigate the combustion behaviour of the fuel at 1600 rpm and 6.5 bar IMEP in a conventional premixed port injection of biogas along with the direct injection of neat Diesel. The 1600 rpm was the optimum speed selected based on the previous test result. Similarly, the 6.5 bar IMEP was the maximum engine load, which indicated an upper maximum temperature expected to improve the combustion attributes compared to the other engine loads. Please refer to article[22] for a detailed procedure. The diesel injection time was advanced to 21° CA BTDC (before the top dead centre) to improve the cylinder mixing and fuel combustion at this load range[26].

Diesel injected in a conventional combustion method was reduced by about 60% at full load[22]. The injected fuel quantity was determined at full load then recorded as the

high reactivity fuel (HRF) fraction for the RCCI combustion. A replaceable biogas fraction was subsequently determined. At the fixed engine speed and load, 40 – 70% biogas fractions at an interval of 10% were introduced to the cylinder through the air intake manifold for 25, 35, and 45% CO_2 proportions.

An average of twelve cycles was taken for the systematic uncertainty error analysis in the combustion data. Generally, the procedure outlined by Barik and Murugan[27] was used to measure the experimental repeatability of the work.

Table 1. Some technical information on the test engine.

Parameters	Details
Model/Type	L100V/4-Stroke, Air-cooled
No. of cylinder	One (1)
Bore/Stroke	86/75 mm
Displacement	435 cm^3
Compression ratio	20.0 ± 0.3
Injection timing	21° CA BTDC
Maximum Rating	3600rpm, 6.8 kW
Injection pressure	200 bar

3.3 Fuels used for the test

The work examines Euro 2M diesel's workability, obtained from the PETRONAS Research Center (PRC), as pilot injected fuel in RCCI mode. The port injected low reactivity fuel (LRF) is synthesized low-grade biogas constituting 25, 35, and 45% CO_2 mole wise, with the balance as CH_4, to simulate biomass-based biogas fuel. The properties of the fuel are shown in Table 2.

Table 2. Properties of the biogases used for the experiment.

Parameter	Biogas 1	Biogas 2	Biogas 3	Diesel
Proportion by mole	25% CO_2	35% CO_2	45% CO_2	
Fuel density (kg/m^3)	1.353	1.563	1.772	820 - 832
Lower flammability limit (mol%)	6.1 – 22.4	6.9 – 25.4	8.3 – 30.3	0.6 – 7.5
Lower heating value (MJ/m3)	26.24	23.15	19.35	36.0
Octane number	>130	>130	>30	
Stoichiometric A/F ratio	14.72:1	13.64:1	12.13:1	15.05:1

4. Results and Discussion

4.1 Ignition and combustion mechanisms of diesel/biogas in RCCI mode

Cylinder temperature, pressure, and heat release are essential factors in explaining the fundamentals of ignition and burning Diesel/Biogas in RCCI mode.

4.1.1 In-cylinder temperature characteristics

Fig. 2a shows that the cylinder temperature development begins before diesel injection because of the air intake temperature and compression. At the injection stage, the temperature reaches 120 to 250 K, depending on the CO_2 concentration. A 45% CO_2 biogas demonstrated the highest temperature at this stage, while 35% CO_2 indicated the least temperature. The temperature differences at the injection period could be due to the variability of the air intake temperature, rate of premixing, and likely diesel impingement. A steadily raised temperature was observed as the piston approached the top dead centre (TDC) and reached 680 to 750 K at TDC, depending on the CO_2 fraction in the biogas. Attaining diesel autoignition temperature of about 482 K occurs around 6 – 10° CA BTDC indicates ignition was initiated in some reactivity pockets but no adequate combustion. At low temperatures, the kinetic of diesel combustion dominates the cylinder until attaining a critical temperature, after which the biogas may abruptly ignite. Subsequently, a critical temperature of 1000 – 1100 K was reached around 10° CA ATDC. At this temperature range, the whole mixture ignites and results in high flame temperature.

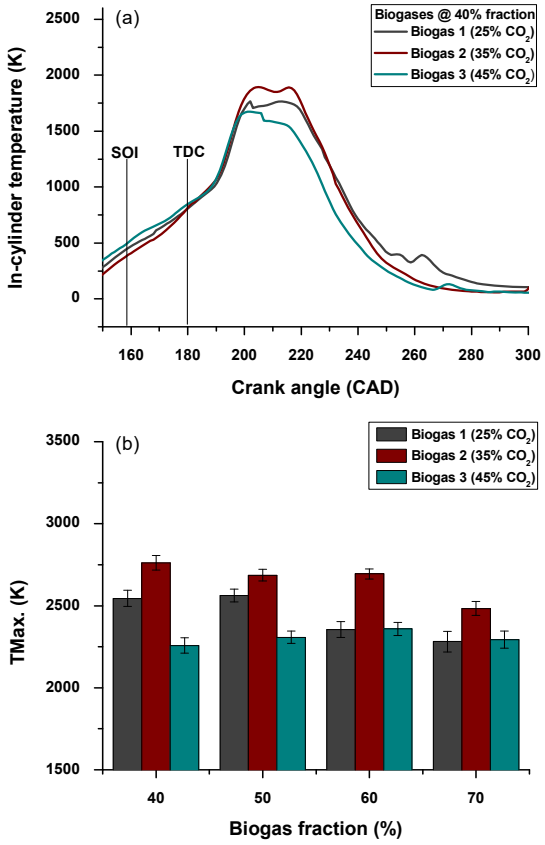

Fig. 2: (a) Temperature traces for biogas/diesel RCCI combustion at 40% fraction and various CO_2 and (b) maximum temperature at different fractions and CO_2 concentrations.

At around 10 – 20° CA ATDC, CO_2 inhibits the combustion, thereby reducing the flame temperature. As observed in Fig. 2a, the temperature production rate drastically reduces with the use of 45% CO_2 compared to

the rest, though 35% CO_2 demonstrates the highest peak temperature. The temperature decrement could be due to the radiation absorption effect of elevated CO_2 concentration resulting in significant energy absorption from the reaction because of high specific heat[17]. This characteristic implies that biogas combustion kinetic dominates the cylinder amidst expansion, making the biogas a primary power source. The case of 25% CO_2 having a lower temperature than 35% CO_2 at the combustion peak might relate to thermal diffusivity change in the flame. A notable decrease in the cylinder temperature was observed at the post flame stage as the CO_2 ratio increases. The enhanced radiation of the CO_2 facilitates heat distribution along the combustion zones[19].

4.1.2 In-cylinder pressure characteristics

The pressure trace for 25% CO_2 depicted in Fig. 3a (1) rises a few degrees before injection due to compression and steadily increases to the end of the compression across biogas. The manifestation of the variability in the pressure traces began around 4° CA ATDC. This phenomenon implies no significant pressure increase due to the abrupt burning before the end of compression because of the reduced diesel amount, which might be insufficient to expand the mixture after ignition. Another factor could be a low temperature due to the cooling effects of the CO_2, as discussed in Section 4.1.1 above. As the pressure variability appears, Fig. 3a (1) shows a drop in the pressure with the increased biogas fraction from 40 to 70% for a 25% CO_2 ratio, especially at the peak stages. The pressure trends for the 25% CO_2 indicate two peaks for all the biogas fractions, as similarly reported by Mikulski and Wierzbicki[28].

The first peak decreases with the increased biogas fraction from 40 to 60% and behaves otherwise at 70% fraction because of reduced diesel amount. Similarly, the second pressure peak for the 25% CO_2 decreases as the biogas fraction increases. The decreasing rate can be seen more pronounced at the second peak than the first for all the fractions. At higher biogas fractions, the reactive mixture quality was substantially reduced by the low heating value of biogas and increased CO_2 concentration. For a 40% biogas fraction, a combined influence of higher diesel amount and CH_4 fraction might improve the pressure growth. As CO_2 concentration increases to 35 and 45%, the pressure traces remain relatively like 25% at all the combustion stages shown in Fig. 3b (1). The second peak drops as the CO_2 ratio increases for the 40% biogas fraction. These variabilities inform that the later peak elevation has no definite pattern relative to high-CO_2 in the mixture.

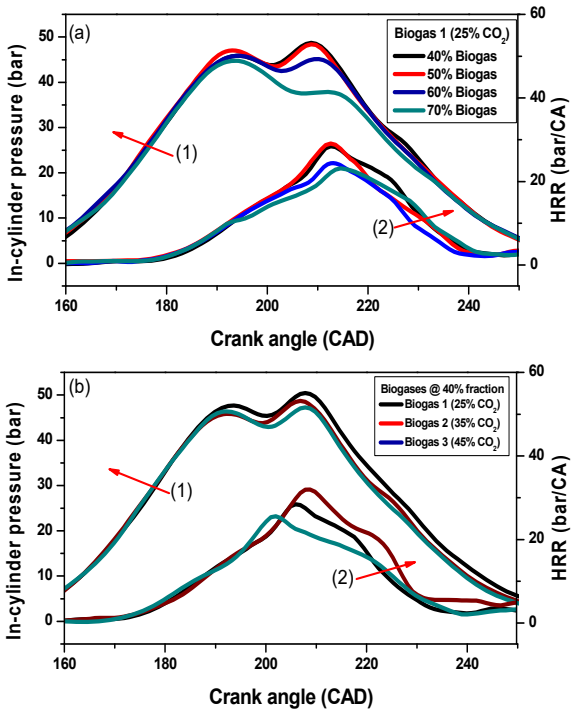

Fig. 3: (a) Trends of the cylinder pressure for 25% CO_2 at various fractions, (b) 40% biogas fraction at different CO_2 levels.

4.1.3 Analysis of the cylinder heat propagation

Fig. 3a (2) shows that the significant heat rise began around 6 – 8° CA BTDC and steadily propagated for a period of 8 – 9 degrees to the end of compression for all the fractions in 25% CO_2 biogas. The heat could relate to diesel autoignition in some reactivity pockets. As discussed in Section 4.1.2, the heat was released, causing elevated pressure but insufficient to cause a significant flame before TDC. The absence of substantially raised heat at this stage could be due to the premixed diluted biogas that absorb most radiated heat. The steadily rise heat propagation began to decline immediately after TDC, indicating more of the cooling effect of the CO_2 due to the burning of biogas, which partakes and inhibits the combustion. It implies that a critical temperature was reached to initiate the second stage ignition and subsequent burning of the whole mixture at this stage. Fig. 3a (2) indicates that 40% and 50% fractions demonstrate the highest peak of the heat than other portions. The similar peak heat by the traces could be attributed to a constant temperature. However, a 40% fraction indicates a bit broader heat distribution as the flame progresses to some degrees. The lowest peak of the heat released appears at 70%, due to an increased radiation absorption effect as the biogas fraction increases. Increasing the CO_2 proportion to 35% demonstrates a trend like 25% except for the 50% biogas fraction, as shown in Fig. 4a. At the main combustion stage, the peak heat released at 50% fraction dropped lower than the discharge of 40 and 60%

fractions. At high temperatures, methyl radicals recombine and inhibit the combustion in the presence of elevated CO_2 [10]. Extending the CO_2 proportion to 45% indicated similar attributes at biogas fractions of 50 to 70% compared to 35% CO_2, shown in Fig. 4b. According to Fig. 3b (2) above, an increased CO_2 proportion decreases the heat release rate due to a reduced temperature because of the radiation absorption effect of high CO_2.

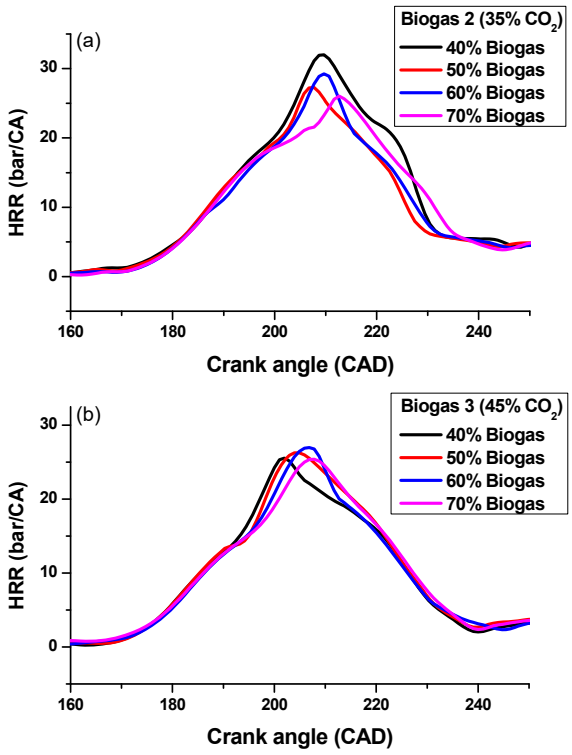

Fig. 4: Heat release rate (HRR) for diesel/biogas RCCI combustion at different fractions for; (a) 35% CO_2, (b) 45% CO_2.

4.2 Combustion magnitude and efficiency of the reactivity fuels

Understanding the combustion variability at different stages is pertinent to explain its magnitude and direction (CA50). As observed in Fig. 5a, 45% CO_2 biogas burned faster than the rest across the fraction, while 25% CO_2 exhibits the slowest burning ability. On average, the first half of fuel got burned at around 18.30° CA (6.353 ms) ATDC while 25 and 35% CO_2 were further slowed by 0.258 and 0.578 ms, respectively. More slowness appears with 40% biogas fraction and decreases as the fraction proceeds to 70% for 25 and 35% CO_2 than the fastest 45% CO_2. According to Zamboni[29], a prolonged burning period slows the combustion centre. Wang et al.[14] reported a slowed burning centre using biogas as LRF in a premixed approach due to atomization of diesel and mixture reactivity.

Specifically, 45% CO_2 indicated a slowed combustion as the biogas fraction increased from 40% to 60%, then fastened as the fraction changes to 70%, which might be due to its lowest burning duration at 70%. The increased biogas fraction slows the combustion averagely by 0.06 ms compared to the reference 40% fraction. Contrarily, an increased biogas fraction speed-up the combustion averagely by 0.097 ms for the 25% CO_2. Similarly, a 35% CO_2 proportion case indicates faster combustion as the fraction increases with an index of 0.38 ms. The 35% CO_2 also demonstrates a lower ignition delay across the fractions except for 40%, as shown in Fig. 6. The lower ignition delay of 35% CO_2 could relate to higher thermal diffusivity due to more temperature developed. A 45% CO_2 that resulted in a fastest burning centre indicates higher ignition delay, unlike 25% CO_2 with moderate ability. As shown in Fig. 5b, combustion efficiency depicts a relatively independent relationship due to increased biogas fraction for 35 to 45% CO_2. Burning a 25% CO_2 demonstrates higher combustion efficiency at 40 to 50% fraction than others. The combustion efficiency increases as the CO_2 increases from 25 to 35%, then decreases as the proportion elevates to 45% across the biogas fractions except for 50%. This trend could be attributed to cylinder heat pattern, though the difference at a 50% fraction proves otherwise.

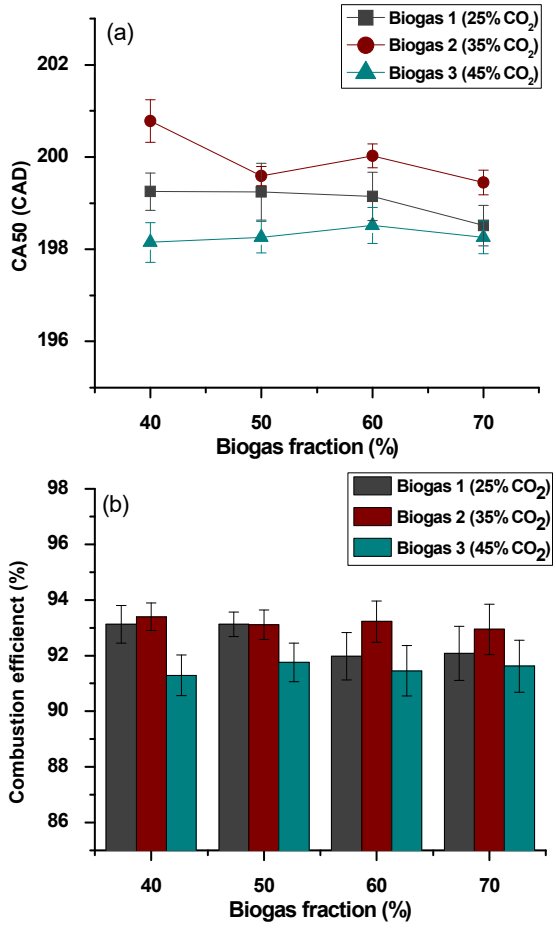

Fig. 5: Variation of; (a) the combustion phasing (CA50) and (b) combustion efficiency for biogas/diesel RCCI combustion at different fractions and CO_2 ratios.

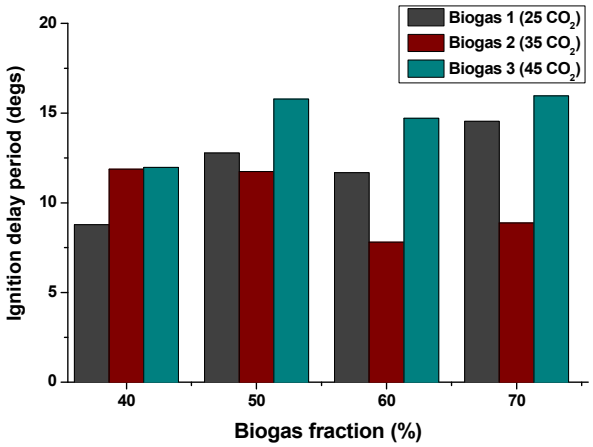

Fig. 6: Variation of ignition delay period for biogas/diesel RCCI combustion at different fractions and CO_2 ratios.

5. Conclusion

An experimental investigation of the influence of CO_2 proportion and biogas fraction on biogas/diesel RCCI combustion behaviour was evaluated at full engine load. The results show that the cylinder temperature across the combustion stages varies with the CO_2 ratios for all the biogas fractions. The radiation absorption effect of high CO_2 concentration reduces the cylinder temperature, causing a delayed expansion to around 10 – 20° CA ATDC, affecting the pressure rise rate at the stage. Both the cylinder temperature and pressure demonstrate a decreasing trend with the increase in CO_2 proportion and biogas fraction. A 35% CO_2 indicates the highest peak pressure at a biogas fraction of 50% with a better heat released, which best performed in biogas/diesel reactivity. A 45% CO_2 composition resulted in delayed ignition but fastest combustion, with the combustion phasing at 6.353 ms ATDC while 25 and 35% CO_2 were slowed by 0.258 and 0.578 ms, respectively. Detailed kinetics mechanisms should be applied to the experimental outcome to understand these fuels' combustion phenomena better.

Acknowledgements

The authors would like to acknowledge the Universiti Teknologi PETRONAS (UTP) support and Centre for Automotive Research and Electric Mobility (CAREM) in conducting this research.

Nomenclature

ATDC	after top dead centre
BTDC	before top dead centre
CA	crank angle
CA50	combustion phasing
CAREM	centre for automotive research and electric
CH4	methane gas
CO	carbon monoxides
CO2	carbon dioxide
H2	hydrogen gas
HRF	high reactivity fuel
IMEP	indicated mean effective pressure
LRF	low reactivity fuel
N2	nitrogen gas
PRC	PETRONAS research centre
RCCI	reactivity controlled compression ignition
TDC	top dead centre
UTP	Universiti Teknologi PETRONAS

References

1) C. A. Cardona, and A. A. Amell. "Laminar burning velocity and interchangeability analysis of biogas/C 3H8/H2 with normal and oxygen-enriched air" *Int. J. Hydrogen Energy* **38**, 7994–8001 (2013).
2) I. B. Dalha, M. A. Said, Z. A. Abdul Karim, M. El-adawy "Effects of port mixing and high carbon dioxide contents on power generation and emission characteristics of biogas-diesel RCCI combustion" *Appl Therm Eng*, **12** (6) 639-649 (2021). https://doi.org/10.1016/j.applthermaleng.2021.117449
3) M. A. Said, I. B. Dalha, M. A. Said, Z. A. Abdul Karim, M. El-adawy "Influence of biogas mixing parameters on the combustion and emission characteristics of diesel RCCI engine" *Alexandria EngJ*,**x**(x)xxx-xxx(2021). https://doi.org/10.1016/j.aej.2021.06.052
4) I. B. Dalha., M. A. Said, Z. A. A. Karim, and F. Firmansyah "Strategies and methods of RCCI combustion: A review" in AIP Conference Proceedings 2035 vol. 030006 030006-1–5 (2018).
5) J. Benajes, S. Molina, A. García, E. Belarte, M. Vanvolsem "An investigation on RCCI combustion in a heavy-duty diesel engine using in-cylinder blending of diesel and gasoline fuels" *Appl Therm Eng* **63** (1) 66–76(2014). http://dx.doi.org/10.1016/j.applthermaleng.2013.10.052
6) Firmansyah, A. A. Aziz, M. Heikal, A. E. Zainal "Diesel/CNG Mixture Autoignition Control Using Fuel Composition and Injection Gap" *Energies* **10** (10) 1639 (2017). http://www.mdpi.com/1996-1073/10/10/1639
7) F. Z. Aklouche, K. Loubar, A. Bentebbiche, S. Awad, M. Tazerout "Experimental investigation of the equivalence ratio influence on combustion, performance and exhaust emissions of a dual fuel diesel engine operating on synthetic biogas fuel" *Energy Convers Manag* **152** (August) 291–9 (2017). http://dx.doi.org/10.1016/j.enconman.2017.09.050
8) B. J. Bora, and U. K. Saha "Experimental evaluation of a rice bran biodiesel e biogas run dual fuel diesel

engine at varying compression ratios" *Renew Energy* **87** 782–90 (2016). http://dx.doi.org/10.1016/j.renene.2015.11.002

9) M. Ayadi, S. Ahou, S. Awad, and Y. Andres "Production of Biogas from Olive Pomace Production of Biogas from Olive Pomace" *Evergreen* **7**, 228–233 (2020).
10) R. Kadam, and N. L. Panwar "Recent advancement in biogas enrichment and its applications" *Renew Sustain Energy Rev* **73** (September) 892–903 (2017). http://dx.doi.org/10.1016/j.rser.2017.01.167
11) O. Mathieu, M. M. Kopp, E. L. Petersen "Shock-tube study of the ignition of multi-component syngas mixtures with and without ammonia impurities" *Proc Combust Inst* **34** (2) 3211–8 (2013). http://dx.doi.org/10.1016/j.proci.2012.05.008
12) M. Fischer, and X. Jiang "An investigation of the chemical kinetics of biogas combustion" *Fuel* **150** 711–20 (2015). http://dx.doi.org/10.1016/j.fuel.2015.01.085
13) M. Fischer, and X. Jiang "An assessment of chemical kinetics for bio-syngas combustion" *Fuel* **137** 293–305 (2014). http://dx.doi.org/10.1016/j.fuel.2014.07.081
14) D. A. Sugeng, W. J. Yahya1, A. M. Ithnin, B. H. Kusdi, M. A. A. Rashid, I. Bahiuddin, N. A. Mazlan, H. A. Kadir "Experimental Comparison of Smoke Opacity and Particulate Matter Emissions with the Use of Emulsion Fuel" *Evergreen* 7, 452–457 (2020).
15) X. Wang, Y. Qian, Q. Zhou, and X. Lu X "Modulated diesel fuel injection strategy for efficient-clean utilization of low-grade biogas" *Appl Therm Eng* **107** 844–52 (2016).http://dx.doi.org/10.1016/j.applthermaleng.2016.07.057
16) Y. Qian, Y. Zhang, X. Wang, X. and Lu X "Particulate matter emission characteristics of a reactivity-controlled compression ignition engine fueled with biogas/diesel dual fuel" *J Aerosol Sci* **113** (August) 166–77 (2017). http://dx.doi.org/10.1016/j.jaerosci.2017.08.003
17) A. Kakaee, P. Rahnama, and A. Paykani "Influence of fuel composition on combustion and emissions characteristics of natural gas/diesel RCCI engine" *J Nat Gas Sci Eng* **25** (x) 58–65 (2015).
18) M. A. Budihardjo, N. Yuliastuti, and B. S. Ramadan "Assessment of Greenhouse Gases Emission from Integrated Solid Waste Management in Semarang City , Central Java , Indonesia" *Evergreen* **8**, 23–35 (2021). http://dx.doi.org/10.1016/j.jngse.2015.04.020
19) S. Abikusna, B. Sugiarto, and I. Yamin "Analysis of utilization low grade bioethanol and oxygenated additives to COV and specific fuel consumption on SI engine" *Evergreen* **7**, 43–50 (2020). http://dx.doi.org/10.1063/5.0014566
20) S. E. Hosseini, M. A. Wahid "Biogas utilization: Experimental investigation on biogas flameless combustion in lab-scale furnace" *Energy Convers Manag* **74** 426–32 (2013). http://dx.doi.org/10.1016/j.enconman.2013.06.026
21) F. M. Quintino, and E. C. Fernandes "Analytical correlation to model diluent concentration repercussions on the burning velocity of biogas lean flames: Effect of CO_2 and N_2" *Biomass and Bioenergy* **119** (September) 354–63 (2018). https://doi.org/10.1016/j.biombioe.2018.09.034
22) I. B. Dalha, M. A. Said, Z. A. A. Karim, E. M. Salah "An Experimental Investigation on the Influence of Port Injection at Valve on Combustion and Emission Characteristics of B5/Biogas RCCI Engine" *Appl Sci.* **10** (452) 1–25 (2020).
23) L. Tarabet, K. Loubar, M. S. Lounici, K. Khiari, T. Belmrabet, M. Tazerout "Experimental investigation of DI diesel engine operating with eucalyptus biodiesel/natural gas under dual fuel mode" *Fuel* **133** 129–38 (2014).
24) W. Guan, H. Zhao, Z. Ban, T. Lin "Exploring alternative combustion control strategies for low-load exhaust gas temperature management of a heavy-duty diesel engine" *Int J Engine Res* **20** 381–92 (2019).
25) M. Vojtíšek, M. Kotek "Estimation of Engine Intake Air Mass Flow using a generic Speed-Density method" *J Middle Eur Constr Des Cars* **12** 7–15 (2015).
26) Y. Wang, M. Yao, T. Li, W. Zhang, and Z. Zheng "A parametric study for enabling reactivity-controlled compression ignition (RCCI) operation in diesel engines at various engine loads" *Appl Energy* **175** 389–402 (2016). http://dx.doi.org/10.1016/j.apenergy.2016.04.095
27) D. Barik, and S. Murugan, "Experimental investigation on the behavior of a DI diesel engine fueled with raw biogas e diesel dual fuel at different injection timing" *J. Energy Inst.* **89** 373–388 (2016).
28) M. Mikulski, and S. Wierzbicki "Numerical investigation of the impact of gas composition on the combustion process in a dual-fuel compression-ignition engine" *J. Nat. Gas Sci. Eng.* **31** 525–537 (2016).
29) G. Zamboni "Influence of fuel injection, turbocharging and EGR systems control on combustion parameters in an automotive diesel engine" *Appl Sci.* **9** (3) (2019).